A B-spline Panel Method using NURBS Surfaces

Boo-Ki Kim and Jong-Ho Nam
Department of Naval Architecture and Marine Engineering
The University of Michigan
Ann Arbor, Michigan, USA

1 Introduction

Panel methods have been extensively used for analyzing potential flows in aerodynamic and hydrodynamic applications. Based on surface description and unknown function representation, we can outline two approaches in panel methods: low-order and higher-order. The low-order (first-order) panel method uses planar triangular and quadrilateral panels having constant values of singularity strength, e.g. Hess & Smith method. This method has been successful for the vast majority of potential flows. In attempting to achieve equivalent accuracy for smaller number of panels, higher-order panel methods have been proposed. For example, Hess (1979) used paraboloidal panels with linearly varying source and vorticity density. A different kind of higher-order method employs quadratic or cubic Lagrangian interpolation functions to represent panel geometry and behavior of potential and its normal derivative over each panel. The higher-order methods are known to be remarkably accurate and efficient compared to the low-order method but retain some drawbacks: (1) in Hess method, the use of cubic panel shape with quadratic source density seems not to be feasible due to the great increase of complexity, (2) the higher-order method using Lagrangian interpolation functions gives the discontinuous normal vector and spatial derivatives of the potential across the panel boundaries. To remedy these drawbacks, we introduce a higher-order panel method using B-splines.

B-spline curves and surfaces have become a standard for geometry description in computer aided design systems. Panel methods using B-spline basis functions, however, have not been thoroughly investigated in fluid problems. Recently, the applications in two-dimensional problems (Hsin *et al.*, 1993) and three-dimensional problems (Ushatov *et al.*, 1994; Maniar, 1995) have been reported. They used the non-rational B-splines for surface representation. Unlike the previous B-spline panel methods, the proposed method in this work features the use of non-uniform rational B-spline (NURBS) surfaces to accommodate more precise geometric representation of given bodies. As a result, the method provides the accurate representation of geometry of bodies, especially bodies with conics; thus gives significant improvements in solving a boundary integral equation.

2 B-spline Panel Method

With assumptions that the fluid is inviscid and incompressible, and that the fluid motion is irrotational, there exists a velocity potential ϕ which satisfies the Laplace equation. The Laplace equation can be transformed into an integral equation by Green's theorem in the second form:

$$C(p)\phi(p) = \int\int_S \left[\phi(q)\frac{\partial G(p;q)}{\partial n_q} - G(p;q)\frac{\partial \phi(q)}{\partial n_q}\right] dS \tag{1}$$

where $C(p)$ is a solid angle at a point $p(x,y,z)$; S represents boundary surface; $\frac{\partial}{\partial n_q}$ is the normal derivative with respect to a point $q(\xi,\eta,\zeta)$ on S. In an unbounded fluid problem, the harmonic function G is expressed as $1/R = 1/\sqrt{(x-\xi)^2+(y-\eta)^2+(z-\zeta)^2}$.

To solve the boundary integral equation (1), the geometry of a body is modeled by the NURBS surface of degree p in u and degree q in v:

$$\boldsymbol{Q}(u,v) = (x(u,v), y(u,v), z(u,v)) = \frac{\sum_{i=1}^{N}\sum_{j=1}^{M} w_{ij}\boldsymbol{P}_{ij}B_i^p(u)B_j^q(v)}{\sum_{i=1}^{N}\sum_{j=1}^{M} w_{ij}B_i^p(u)B_j^q(v)} \tag{2}$$

where w_{ij} is the weight; $\boldsymbol{P}_{ij}$ is the net of control points; $B_i^p(u)$ and $B_j^q(v)$ are the B-spline basis functions defined on the knot vectors in u and v parametric directions, respectively; and N and M are the number of control points in the u and v directions, respectively. Further, ϕ and $\frac{\partial\phi}{\partial n_q}$ are assumed as

$$\phi(u,v) = \sum_{i=1}^{n}\sum_{j=1}^{m} a_{ij}B_i^k(u)B_j^l(v) \tag{3}$$

$$\frac{\partial\phi}{\partial n_q}(u,v) = \sum_{i=1}^{n}\sum_{j=1}^{m} b_{ij}B_i^k(u)B_j^l(v) \tag{4}$$

where a_{ij} and b_{ij} are nets of control points for the potential and its normal derivative over the body surface, respectively; $B_i^k(u)$ and $B_j^l(v)$ are the B-spline basis functions of degree k in u and degree l in v; and n and m are number of control points in the u and v directions, respectively.

To obtain the numerical solution, the body surface is discretized into number of panels. The parametric coordinates u and v of the knots are divided into n and m points, respectively, resulting in $(n-1)\times(m-1)$ rectangular segments in the parametric domain. Each segment corresponds to the surface panel in the physical domain. Then the collocation at the corner points of each panel results in the linear system of equations with $n \times m$ unknowns. The control net a_{ij} for the potential or b_{ij} for the normal derivative of the potential are the unknowns to be determined, depending on the type of given boundary conditions. The influence coefficients by source and normal dipole terms are evaluated using the PART (Projection and Angular & Radial Transformation) method for the near field, Telles (1987) method for the intermediate field, and 6 × 6 Gauss quadrature integration for the far field. Hayami and Matsumoto (1994) suggested this strategy for the choice of the efficient numerical method to integrate influence functions. The PART method noticeably reduces the number of integration points for singular integrals compared to the polar coordinate transformation method which has been commonly used. The linear system of equations is solved using the LU decomposition method.

3 Numerical Results

To perform numerical computations, we consider a uniform flow past a sphere in an unbounded fluid. For simplicity, the radius of the sphere is taken to be 1 and the onset flow is from the -x-direction with its velocity U=1. The sphere is represented exactly by the bi-quadratic NURBS surface with 45 ($N = 9, M = 5$) control points. The weights and non-uniform knot vectors can be found in Rogers and Adams (1990). The surface is discretized into the a set of panels by equal spacing in u and v parameters. Due to the flow symmetry, one-eighth of the sphere surface is modeled.

For the verification of the accuracy of the sphere defined by NURBS surface, the unit normal vectors and surface area are investigated. As expected, the calculated unit normal vectors are exactly equal to the analytical results. As shown in Figure 1, the NURBS technique is superior to other

methods for calculating the surface area.

In exterior Neumann problems, it is noted that the control points a_{ij} for the potential are the remaining unknowns in the linear system of equations because $\frac{\partial \phi}{\partial n_q}$ is given by the body boundary condition. The bi-linear, bi-quadratic, and bi-cubic B-splines with uniform knots are used for the potential variation over the body surface. Figure 2 shows the RMS error, defined by $\sqrt{\sum_{i=1}^{n \times m}[(\phi)_{analytic} - (\phi)_{calculated}]^2/(n \times m)}$, in the potential evaluated at the collocation points while increasing the number of panels. It is seen that the RMS error can be greatly reduced as the number of unknowns increases. Figure 3 and 4 show potential and pressure distributions along the polar angle θ=0^o (stagnation point) to θ=90^o at the y=0 plane on the sphere surface, respectively. The computed results are in excellent agreement with the analytical solutions. The absolute errors in the drag force acting on the front half of the sphere are plotted in Figure 5. The analytic value is $C_x = \frac{-\int\int p n_x dS}{1/2 \rho S U^2}$ = -0.0625, where ρ is the fluid density, S is the surface area, p is the pressure, and n_x is the x-component of the unit normal vector directed into the fluid region. The method using the cubic potential spline shows a rapid decrease in error and good convergence with the increasing number of panels. Overall, the method based on B-splines gives better results than Hess method. Figure 6 shows the absolute errors in the added mass of the sphere translating in an unbounded fluid. The analytic value is $\int\int \phi n_x dS = \frac{2\pi}{3}$. The bi-cubic potential spline appears to converge faster than bi-linear and bi-quadratic ones. This observation is similar to the one obtained from Figure 5.

4 Concluding Remarks

A three-dimensional higher-order panel method using B-splines has been developed to solve a boundary integral equation in potential flow problems. Specially, the NURBS technique was introduced for exact geometric representation. The improvements for obtaining accurate solutions by the proposed method have been demonstrated. The application of the method to free-surface flow problems remains for future study.

References

Hayami, K. and Matsumoto, H., 1994, "A numerical quadrature for nearly singular boundary element integrals," *Engineering Analysis with Boundary Elements*, **13**, pp. 143-154.

Hess, J.L., 1979, *A Higher Order Panel Method for Three-Dimensional Potential Flow*, Report No. NADC-77166-30.

Hsin, C.-Y., Kerwin, J.E. and Newman, J.N., 1993, "A higher-order panel method based on B-splines," *Proceedings* of the 6th International Conference on Numerical Ship Hydrodynamics.

Maniar, H., 1995, *A Three Dimensional Higher Order Panel Method based on B-Splines*, Ph.D. thesis, Massachusetts Institute of Technology.

Rogers, D.F. and Adams, J.A., 1990, *Mathematical Elements for Computer Graphics*, McGraw-Hill Publishing Company, Second Edition.

Telles, J.C.F., 1987, "A self-adaptive co-ordinate transformation for efficient numerical evaluation of general boundary element integrals," *International Journal for Numerical Methods in Engineering*, **24**, pp. 959-973.

Ushatov, R., Power, H. and Rego Silva, J.J., 1994, "Uniform bicubic B-splines applied to boundary element formulation for 3-D scalar problems," *Engineering Analysis with Boundary Elements*, **13**, pp. 371-381.

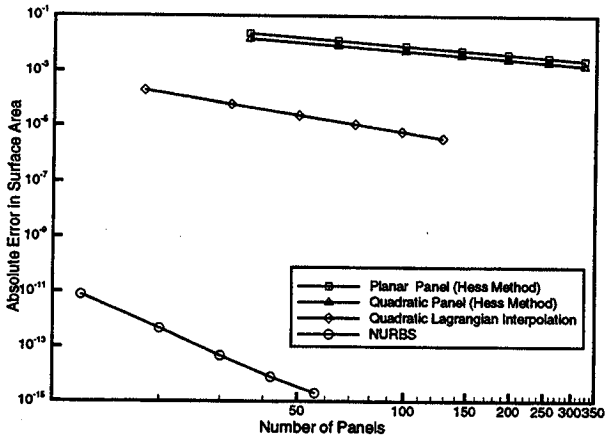

Figure 1: Absolute error in surface area

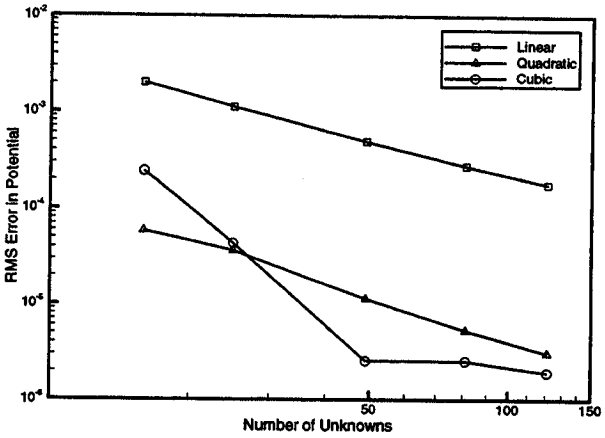

Figure 2: RMS error in potential

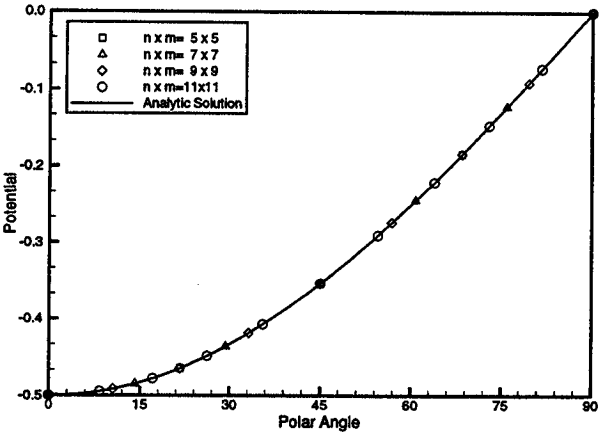

Figure 3: Potential on the sphere surface

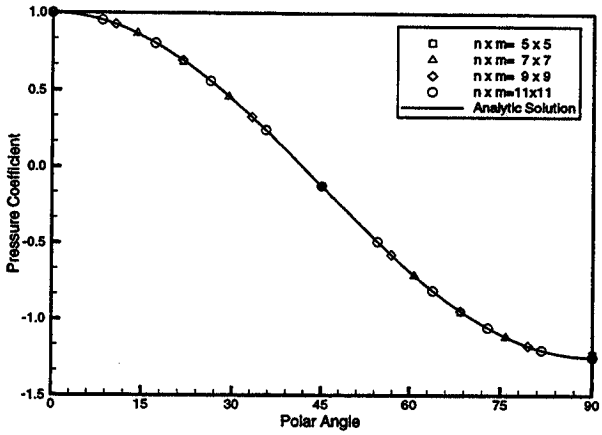

Figure 4: Pressure on the sphere surface

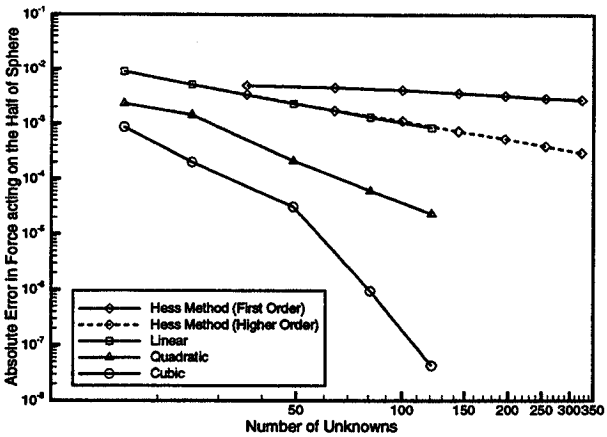

Figure 5: Absolute error in drag force acting on the half of the sphere

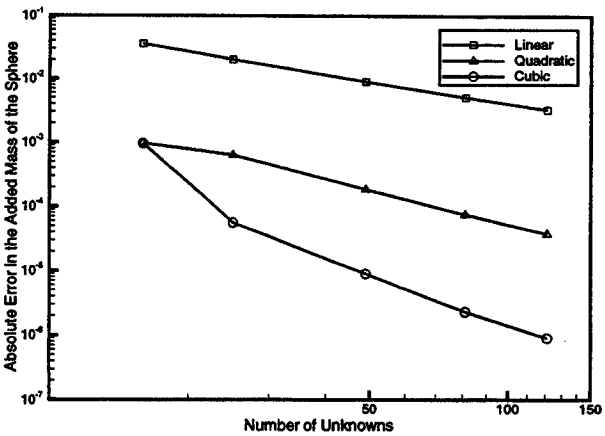

Figure 6: Absolute error in the added mass of the sphere